CIRP Annals - Manufacturing Technology 00 (2023) 1–4

Contents lists available at ScienceDirect

CIRP Annals - Manufacturing Technology

journal homepage: https://www.editorialmanager.com/CIRP/default.aspx

Large-scale metal strip for power storage and energy conversion applications by machining-based deformation processing

James B. Mann[a], Debapriya P. Mohanty[b], Andrew B. Kustas[c], B.Stiven Puentes Rodriguez[b], Mohammed Naziru Issahaq[b], Anirudh Udupa[d], Tatsuya Sugihara[e], Kevin P. Trumble[b], Rachid M'Saoubi (1)[f,g,*], Srinivasan Chandrasekar[b]

[a] M4 Sciences Corporation, Lafayette, IN, USA
[b] Center for Materials Processing and Tribology, Purdue University, West Lafayette, IN, USA
[c] Material, Physical, and Chemical Sciences Center, Sandia National Laboratories, Albuquerque, NM, USA
[d] Department of Mechanical Engineering, BITS Pilani, Hyderabad, India
[e] Department of Mechanical Engineering, Osaka University, Osaka, Japan
[f] R&D Material and Technology Development, Seco Tools AB, Fagersta, Sweden
[g] Department of Mechanical Engineering Sciences, Division of Production and Materials Engineering, Lund University, Lund, Sweden

ARTICLE INFO

Article history:
Available online xxx

Keywords:
Machining
Sheet metal
Energy efficiency

ABSTRACT

Machining-based deformation processing is used to produce metal foil and flat wire (strip) with suitable properties and quality for electrical power and renewable energy applications. In contrast to conventional multistage rolling, the strip is produced in a single-step and with much less process energy. Examples are presented from metal systems of varied workability, and strip product scale in terms of size and production rate. By utilizing the large-strain deformation intrinsic to cutting, bulk strip with ultrafine-grained microstructure, and crystallographic shear-texture favourable for formability, are achieved. Implications for production of commercial strip for electric motor applications and battery electrodes are discussed.

1. Introduction

Thin-gauge strip (foil, sheet and flat wire formats) of Al, Cu and electrical steels are critical for power storage and renewable energy applications, including electrical conductor wire, high-performance motor windings and core laminations, and electric vehicle (EV) battery electrodes. Today, virtually all commercial metal strip is produced by multistage deformation processing (rolling or drawing), wherein large thickness reductions often require up to 30 stages of incremental deformation. These traditional manufacturing processes are capable of large-volume production. However, they are multi-step, energy intensive, and inflexible, posing constraints to product design and performance – especially in materials for EVs and next-generation motors. With steel sheet products, for example, the rolling energy consumption is second only to that of blast furnace operations [1,2]. Furthermore, rolled-strip cost increases near-exponentially with decreasing size into foil range [3]. It is therefore of interest to develop new alternative processes for strip production – particularly in speciality applications. In this study, we show, using diverse examples, that large-scale strip production by machining-based deformation processing is a possible process solution.

2. Background: shear-based deformation processing

Chip formation is a large-strain deformation process involving action of a tool against a workpiece (Fig. 1). The chip, the process end-product in the present study – in sheet, flat wire or foil form – is created by feeding the tool, with rake angle (γ), radially into a rotating workpiece at specified undeformed chip thickness, h_o. A continuous strip of thickness $h_c > h_o$, is produced at speed V_0 by intense shear confined to a narrow shear zone AB. Conventional (free) machining (without the constraint in Fig. 1) is called FM to emphasize that the exit chip thickness (h_c) is not set *a priori*, but is an output of the deformation process. The chip formation can be converted into a strip-forming process – hybrid cutting extrusion (HCE), with h_c set *a priori* – by using a second constraining die located across from the primary tool, see Fig. 1 [4,5].

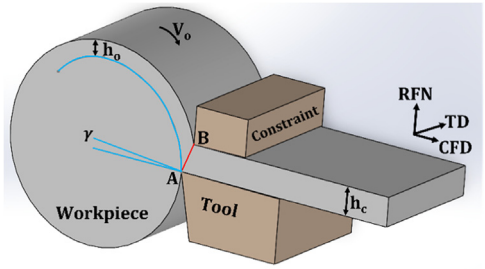

Fig. 1. Shear-based deformation processing in plane-strain by HCE. RFN, TD and CFD represent directions parallel to rake face normal, chip width (transverse) and chip flow, respectively.

* Corresponding author.
E-mail address: rachid.msaoubi@secotools.com (R. M'Saoubi).

https://doi.org/10.1016/j.cirp.2023.04.084
0007-8506/

In HCE, unlike FM, h_c can be set smaller than h_o [5]. The von Mises strain in the strip is, by the shear plane model, with $\lambda = h_c/h_o$ [4,5],

$$\varepsilon = \frac{1}{\sqrt{3}}\left(\frac{\lambda}{\cos\gamma} + \frac{1}{\lambda\cos\gamma} - 2\tan\gamma\right) \quad (1)$$

The use of chip formation to produce metal strip is not new. It appears to have originated in a process called peeling [6] – cutting with large positive rake angles, as high as 45°, often coupled with chip-tensioning. The earliest (German) patents on the subject date to 1925. Subsequently, constrained cutting processes emerged [4,5,7,8], to produce strip of narrow width – precursors to the current HCE. HCE has unique deformation attributes [5,9]. It can a) provide two-parameter control of deformation path and chip strain, via λ and γ, for control of strip microstructure/texture; b) produce strip with fine-grained microstructures via controlled large-strain deformation; and c) suppress flow instabilities via favourable shear zone conditions (high hydrostatic pressure and adiabatic deformation). These findings suggest that HCE and FM can be developed for production of strip from ingot, in a single step, at scale, for electrical and structural applications. The ensuing examples highlight this transformative potential of HCE and FM for strip production.

3. Results

3.1. Al flat-wire for electrical conductor applications

Al 1100 (> 99% Al) wire is used in electrical conductor applications, because of its high electrical conductivity, low density and capability to be strengthened by cold-working. Rectangular cross-section, flat wire is conventionally produced by rolling/drawing involving 10 to 20 cold-deformation steps. In the annealed (O-temper) condition, the alloy has low strength (UTS < 90 MPa), but high ductility (elongation (EL) > 40%) and electrical conductivity (57 – 62% IACS) [10], see also ASTM-B230/B230M-07. The low strength precludes direct use in the annealed or as-cast condition in most applications. Consequently, strain-hardened tempers, from H12 (1/4 hard) to H18 (full-hard) to H19 (extra-hard), have been developed utilizing deformation processing [10]. Strain hardening is the preferred strengthening mode, as it does not significantly reduce the conductivity. The H18 corresponds to cold rolling reduction of 75%, with ductility of 1–4% EL; while the H19 is the highest commercial strain-hardened temper, with ductility of only 1.2%. We demonstrate HCE processing of Al flat wire – strength > 150 MPa, high electrical conductivity > 56% IACS, and surface quality superior to rolled or drawn wire, in a single process step, from Al 1100-O stock (27 HV).

The wire production used disk workpieces (6 mm thickness x 140 mm diameter) cut from cold-rolled plates in the half-hard (H14) condition, followed by annealing at 300 °C for 2 h. The tests were conducted on a flat-bed lathe (Haas TL-2). Based on preliminary FM experiments, the following HCE conditions were chosen: γ = 20°, h_0 = 0.125 mm, V_0 = 6 m/s, λ of 2.5 with a HSS tool (edge radius ~ 0.005 mm) and dry cutting. Under equivalent conditions, the flat-wire thickness produced in the FM sets the upper limit ($\lambda \sim 5.5$) for HCE wire thickness. Microstructure of the wire was characterized by optical metallography; surface finish by stylus/optical profilometry; and strength by Vickers indentation. Conductivity (%IACS) was determined in line with ASTM standard B193, by resistance measurements on wire of 0.5 to 1 m length.

Fig. 2a shows a coil of flat wire, 0.2 mm thickness, produced by HCE. The ε imposed in the wire was ~ 1.4 (λ = 2.5, Eqn. (1)). The h_c and λ parameters enable independent control of wire strain and thickness, a unique HCE feature not available in rolling. Both the rake face (front) and constraint face (back) in Fig. 2 have smooth shiny surfaces, devoid of material pull-out. Optical profilometry showed the mean Ra on the wire surfaces to be 0.25 μm (rake) and 0.34 μm (constraint). These values are determined by the finish on the cutting tool/constraint tool faces. For reference, Ra for commercial drawn Al flat-wire is 0.8 to 3.3 μm, and for rolled Al is 0.4 to 0.8 μm [10,11]. By varying h_0, continuous flat wire of 6 mm width and 0.2 to 0.9 mm thickness was produced by HCE. With regard to FM wire, while its front surface (in contact with the cutting tool) had a finish similar to HCE wire (from high tool pressure/constraint), the free surface (back) showed visible roughness, from unconstrained material flow. In HCE, the constraint suppresses this out-of-plane flow, enabling a smooth finish also on the wire back surface.

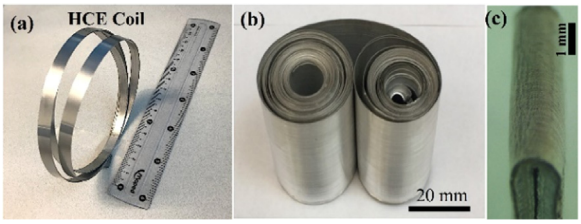

Fig. 2. Flat wire and foil produced by (a) HCE Al 1100 and (b) FM Al6061-T6. Image (c) highlights formability of Al 1100 strip in 0T bend test.

Table 1 gives measured hardness and electrical conductivity for the wire forms. The strain (ε) is estimated using measured thickness reduction for rolling, and chip thickness ratio (Eq. (1)) for HCE. The utility of the shear-based processing in increasing the strength of the wires is evident. The HCE wire strength is ~ 1.7 X that of annealed wire (27 HV), a consequence of the large ε imposed. This strength compares favourably with commercial wire produced by multi-step rolling/drawing (H18). Similar results were seen with wire produced from another Al conductor alloy EC1350 in H19 condition. Despite the large ε, the HCE wire showed surprisingly high formability in standard 0T bend testing [12], see Fig. 2c. At bend radius of "zero", where the wire is flattened onto itself, the maximum circumferential ε is ~ 1.0. But there was no cracking even in 5 repeat trials, at this high ε, due to strong crystallographic shear textures imposed by the processing.

Table 1
Hardness and electrical conductivity of Al 1100 wire.

Condition	strain (ε)	HV	Conductivity (%IACS)
Annealed (O-temper)	0	27 ± 2	57.9 ± 0.2
HCE	1.4	45 ± 1	58.2 ± 0.1
Commercial H18 [10]	1.6	49	57

Table 1 also shows conductivity of the HCE wire to be similar to that of commercial H18 and annealed 1100 wire. This is consistent with the well-established fact that plastic deformation has only a negligible effect on electrical conductivity of metals, in contrast to alloying content. The results illustrate the efficacy of the single-step HCE for producing wire of sufficiently high strength by plastic straining, but without compromising electrical conductivity.

Other experiments showed that FM, when coupled with a follow-on, light cold-rolling (CR) step (20% reduction), could also create wire with similar properties as HCE wire. The light CR step is sufficient to reduce the Ra on the wire back-surface to commercial specifications. Hence, an FM + CR (2-step) process can also be viable for producing commercial-quality wire. Fig. 2b shows 50-mm wide Al alloy strip of 0.1 mm thickness, several meters in length, created by FM+CR using a large HSS tool (edge radius 0.02 mm, dry cutting). The Ra on the wire surfaces was 0.35 to 1 μm, similar to rolled strip. This strip was produced from structural Al6061-T6 (100 HV) to show that the shear-based processing is also applicable for producing foil from higher-strength alloys.

3.2. High-Si electrical steels for motor core laminations

The second strip-production example involves high-Si iron alloys (electrical steels), under consideration for next-generation, electrical motor core laminations. It is well known that Fe-Si alloys, with >3.2% Si content, can improve the efficiency of electrical motors if available in strip form at reasonable cost [13]. A US Department of Energy (DOE) analysis states that approximately 12,000 GWh annual energy savings can be achieved with high-Si steels. While the electromagnetic attributes (resistivity, core loss) of the high-Si alloys for motors are exceptional, these alloys have limited workability, making them difficult to produce in strip forms that can be laminated and stacked for motor cores. Current deformation processing involves multistage rolling, with 20 to 30 steps– incremental hot/cold rolling reductions - interspersed with annealing and cleaning. This processing has important

Please cite this article as: J.B. Mann et al., Large-scale metal strip for power storage and energy conversion applications by machining-based deformation processing, CIRP Annals - Manufacturing Technology (2023), https://doi.org/10.1016/j.cirp.2023.04.084

disadvantages – large energy consumption and emissions, limitations in processing of low-workability, high-Si steels to thin foil form (important for reducing core loss), large-scale plant infrastructure, and limited control of sheet microstructure and crystallographic texture. It is therefore of interest to have an alternative process that can produce high-Si Fe alloy strip while concurrently addressing these deficiencies.

The electrical steel strip demonstration uses Fe-4%Si-4%Cr alloy, with resistivity > 80 μΩ-cm, flux density > 1.48 T at 5000 A/m, and core loss 35% lower than benchmark 3.2% Si alloy. The alloy, designed by the Purdue group, meets US DOE specifications for next-generation motors; the Si and Cr were tailored for electrical properties and material workability, respectively [11]. For the experiments, an ingot was cast by vacuum induction melting and hot forged at ~1200 °C to produce a disk workpiece, 210 mm diameter X 55 mm thickness, and hardness ~ 230 HV.

Experiments were performed on a 30-kW lathe (Okuma LB-4000EXIIBB/750) with special tooling designed for high forces. Fig. 3 shows the integrated HCE tool assembly, and large-scale, 55 mm wide TiN-coated WC-10%Co cutting/constraint tools (edge radius 0.020 mm). The process conditions were γ = 10°, h_0 = 100 μm to 250 μm, V_0 = 0.5 m/s to 6 m/s, and dry cutting. Fig. 3c and d, respectively, show HCE (~20 mm wide, λ = 1.2) and FM+CR (50 mm wide) strips, with nominal thickness of 0.3 mm and 0.225 mm. The CR reduction with the FM strip was 25% to reduce the back-surface roughness. HCE could also produce strip from extremely low-workability Fe-6.5% Si (lowest core loss alloy), an alloy that is near-impossible to cold-roll.

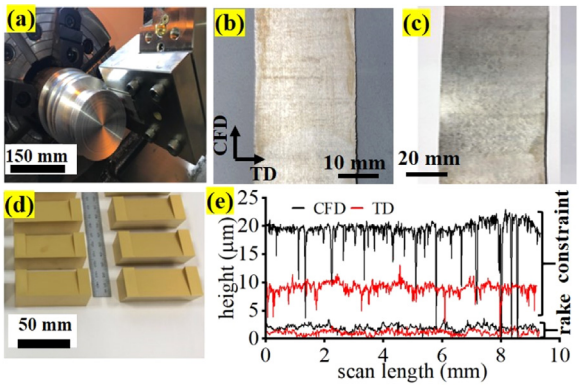

Fig. 3. Fe-4Si-4Cr alloy strip by HCE and FM+CR (a) lathe tool assembly (b) HCE tools (c) HCE strip (d) FM+CR strip; and (e) line profiles from optical profilometry of both surfaces of HCE strip (along CFD and TD).

Fig. 3e shows a line profile from optical profilometry of the front and back HCE strip surfaces. The lay of the surface is along CFD on the rake side and parallel to TD on the constraint face, due to the nature of the primary and secondary deformation features. Both surfaces are quite smooth, with Ra of 0.11±0.03 μm (CFD) and 0.12±0.02 μm (TD), rake surface; and 0.82±0.07 μm (CFD) and 0.41±0.05 μm (TD), constraint surface. The constraint surface is somewhat rougher than the rake surface, as small irregularities on the constraint edge replicated onto the strip surface. The FM+CR strip showed very similar roughness as the HCE strip. The hardness of the strips was 350 to 380 HV, an ~55% strength increase over the initial material (~230 HV). This strengthening is accompanied by loss of ductility, also seen in commercial rolled sheet. Hence, commercial Fe-Si sheet is high-temperature annealed, post-rolling, to recover workability, so that motor core laminations can be stamped out of the sheet without cracking. The HCE Fe-4Si-4Cr strip, after a similar anneal, showed comparable formability as commercial rolled (3% Si) strip in 0T bend testing. The strip could be folded over onto itself as in Fig. 2b without cracking in the outer tensile fibers.

A homogeneous flow-line type microstructure was typical of strip produced by the shear-based processing, with the flow lines aligned in the direction of maximum tensile strain in the chip. The flow line pattern is a macroscopic manifestation of the underlying crystallographic texture, which for the Fe-Si BCC system is well-captured in the Electron Back Scattered Diffraction (EBSD) (101) pole figure. Fig. 4a shows the (101) pole figure in the thickness cross-section (RFN—CFD plane) for Fe-4Si strip (λ = 2, V_o = 2 m/s).

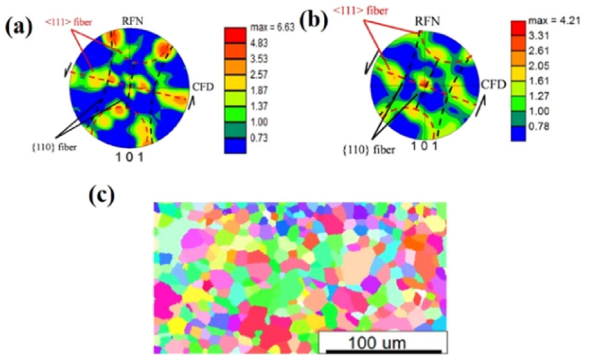

Fig. 4. EBSD analysis of Fe-4Si strip a) (101) pole figure (λ = 2, V_o = 2 m/s). The {110} and ⟨111⟩ shear texture fibers are highlighted by black and red dotted lines, respectively; b) (101) pole figure for strip produced at higher temperature (V_o = 3 m/s, workpiece pre-heat temperature, 300 °C); and c) inverse pole figure map corresponding to b) showing dynamically recrystallized fine-grained microstructure. (For interpretation of the references to colour in this figure legend, the reader is referred to the web version of this article.)

The deformation texture is characterized by two partial {110} and ⟨111⟩ fibers, highlighted by the dotted lines in the figure, that are characteristic of simple-shear BCC textures [14]. The ideal {110} fiber with uniform intensity results from alignment of the (110) plane in a direction parallel to the shear plane; this fiber also reflects orthotropic symmetry around the plane normal. Similarly, the ideal ⟨111⟩ fiber arises from [111] aligning along the shear direction, with orthotropic symmetry around this direction. The angle by which these fibers are rotated (~76°, counter-clockwise to CFD in Fig. 4a) is consistent with the shear plane orientation (80° to the CFD) for this process condition. Given the large strains ($\varepsilon \sim 1$) imposed in the strip, this close alignment of the fibers with the shear direction – a shear texture – is to be expected. The shear texture can be varied via λ and γ, enabling unique texture control, something not possible in rolling. This strong shear texture is likely responsible for the high formability of the strip, both the Al 1100 and high-Si steel, produced by the shear-based processing.

When V_o was increased to 3 m/s, along with workpiece pre-heating to 300 °C, the strip showed a fully recrystallized microstructure with fine grain size of ~8 μm (Fig. 4b, c). Dynamic recrystallization occurred in the shear zone (estimated T ~ 650 °C), even though the material element experienced the high T for only ~100 μs. Furthermore, the texture components in the recrystallized strip are essentially the same as in the parent (strip) deformation texture (Fig. 4). Similar retention of deformation texture was also found after static recrystallization at 700 °C.

The capability of HCE and FM to produce strip from low-workability Fe-Si (3.2 to 6.5% Si), as well as alloys like MgAZ31B and Ti6Al4V, is a consequence of the large hydrostatic pressure, intense shear strain, and adiabatic deformation (heating) conditions in the process zone [5,9,11]. These conditions favor suppression of cracking in low-workability alloys – an outstanding feature of this processing for strip production. Ongoing work is focused on process scaling for strip of 100 to 150 mm width, a size range ideal for small-motor laminations.

3.3. Copper strip for battery electrodes

The final demonstration is large, 105-mm wide Cu strip in discrete lengths. Cu and Al strip of 20 to 600 mm width are of interest for Li-ion battery electrodes. A linear FM configuration on a modified double-column machining center (Hurco BX60i), processed foil of 105 mm width X 0.15 to 0.35 mm thickness from C101 Cu M20 temper (as hot rolled, 68 HV). The workpiece 152 mm thick X 305 mm length X 105 mm was sectioned from rolled plate. FM was done on the 305 mm X 105 mm, with a TiN coated WC—Co tool (edge width 155 mm, radius 0.02 mm), and process conditions: γ = 10°, h_0 = 50 μm, V_o = 0.033 m/s, dry cutting.

In initial experiments, we could not achieve strip production because of significant sinuous flow [15] and fracturing in the deformation zone – a consequence of the highly heterogeneous microstructure of the initial (rolled) workpiece material (across the

Please cite this article as: J.B. Mann et al., Large-scale metal strip for power storage and energy conversion applications by machining-based deformation processing, CIRP Annals - Manufacturing Technology (2023), https://doi.org/10.1016/j.cirp.2023.04.084

thickness). Remarkably, the heterogeneity-driven sinuous flow and fracturing could be suppressed and replaced by chip formation with uniform laminar flow, when the Cu workpiece surface was coated prior to each cut using a permanent marker (Sharpie) [15]. The coating produces an ink film of ~200 nm thickness, that changes the flow mode via a mechanochemical effect on surface plasticity. Strip formation could now be effectively realized. Fig. 5a shows typical FM strip – 105 mm width X 45 mm length, perhaps the widest strip produced by machining-based processing. Because Cu undergoes significant deformation in chip formation, the strip thickness was ~7.5h_0 (λ~7.5), corresponding to ε~4.3. The large straining results in significant grain refinement, with the strip material having an ultrafine-grained (UFG) microstructure – grain size ~0.8 μm (Fig. 5b) – and 2.4X strength increase (strip ~ 160 HV). The 160 HV hardness is close to the maximum value typical of UFG Cu processed by severe plastic deformation. The results are promising for process scale-up; and for processing UFG metals commercially in sheet form, a quest as yet unrealized even for lab-scale property measurements.

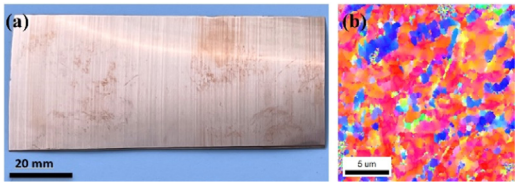

Fig. 5. Shear deformation processing of Cu a) FM strip of 105 mm width; and b) UFG microstructure in strip (RFN-TD thickness section) by EBSD.

4. Energy analysis synopsis

A process energy analysis of HCE and multistage rolling was carried out to determine differences if any in the specific energy between the two types of processing for strip/wire production. For the multistage rolling, we used rolling schedules typical of industrial sheet processing of 316 stainless steel and an Al alloy with mechanical properties analogous to 6061-T6. The schedule used was reduction from initial block thickness of 700 mm to final sheet thickness of 0.5 mm, involving nominally 23 hot rolling passes (to 3.5 mm thickness), followed by 2 cold rolling passes to final 0.5 mm thickness. The hot/cold rolling temperatures were nominally 575 °C/25 °C for the Al alloy; and 1200 °C/25 °C for the 316 SS. Details about deformation modeling, process conditions and material properties may be found in Ref. [11]. The energy was estimated as the sum of the workpiece pre-heating energy and deformation processing energy (via simulation). The principal conclusions were a) the rolling specific energy was ~ 1190 MJ/ton (Al) and ~ 2000 MJ/ton (316SS), and b) that ~ 65% of this energy was due to workpiece pre-heating for the hot rolling. We also estimated the corresponding specific energy for production of 0.5 mm thickness Al alloy strip by HCE, using measured force data. The process conditions were h_o = 0.3 mm, λ = 1.67, V_o = 2 m/s; γ = 5°, and dry cutting. The HCE specific energy was ~ 270 MJ/ton, < 30% of that of the rolling. A similar HCE energy reduction was also predicted for 316 SS strip production. The preliminary analysis suggests that the machining-based processing enables attractive energy savings advantages compared to conventional processing.

5. Summary and implications

Machining-based deformation processing is shown to produce strip with necessary properties and quality for electrical applications. The varied examples presented encompass a range of metal systems and product scale. By controlling the large-strain deformation, bulk strip with UFG microstructures and enhanced strength, and simple shear-textures favourable for formability, are achieved. The specific energy for producing metal strip by the machining-based processing is < 1/3rd that of the rolling. While the production capability of this shear-based processing is not yet fully developed, it offers important advantages over conventional processing, especially for specialty electrical applications. These are production of sheet in a single step from ingot, compact infrastructure (few metres vs a kilometer for rolling), strip from even low-workability alloys, smaller process energy, and potential cost benefits for thin-section formats. Challenges that need to be addressed are tool wear (for cost), process configuration design, and process limits in terms of strip size and production rate.

Declaration of Competing Interest

The authors declare that they have no known competing financial interests or personal relationships that could have appeared to influence the work reported in this paper.

Acknowledgment

We acknowledge Benny Christiansen (Manager, Seco Tools R&D prototyping Lab) for manufacture of the tooling used. The research was supported by US DOE EERE Award DE-EE0007868; and NSF grants CMMI 2100568, DMR 2104745 and PFI 2141180 to Purdue. Additional support was provided by Sandia National Laboratories LDRD office. Sandia National Labs is a multi-mission laboratory managed and operated by National Technology and Engineering Solutions of Sandia, LLC., a wholly owned subsidiary of Honeywell International, Inc., for the U.S. DOE's National Nuclear Security Administration under contract DE-NA-0003525. This paper describes objective technical results and analysis. Any subjective views or opinions expressed in the paper do not necessarily represent the views of the US DOE or the US Government.

References

[1] Fruehan RJ, Fortini O, Paxton HW, Brindle R (2000) Theoretical minimum energies to produce steel for selected conditions. *US OSTI Report* 769470. https://doi.org/10.2172/769470.
[2] Sakamoto Y, Tonooka Y, Yanagisawa Y (1999) Estimation of energy consumption for each process in the japanese steel industry. *Energy Conservation and Management* 40(11):1129–1140.
[3] Froes FH, et al. (2007) Cost-affordable titanium: the component fabrication perspective. *Journal of Metals* 59:28–31.
[4] De Chiffre L (1976) Extrusion-cutting. *International Journal of Machine Tool Design and Research* 16(2):137–144.
[5] Moscoso W, Shankar MR, Mann JB, Compton WD, Chandrasekar S (2007) Bulk nanostructured materials by large strain extrusion machining. *Journal of Materials Research* 22(1):201–205.
[6] Vigor CW, Leibring W (1973) Metal peeling for production of stainless steel foil for gas turbine regenerators. *SAE Transactions* 82(1):435–440.
[7] Shaw MC, Hoshi T (1977) Cut-forming: a new method of producing wires. *ASME* Journal of Engineering for Industry 99(1):225–228.
[8] Green D (1972) Continuous extrusion-forming of wire sections. *Journal of the Institute of Metals* 100:295–300.
[9] Efe M, Moscoso W, Trumble KP, Compton WD, Chandrasekar S (2012) Mechanics of large strain extrusion machining and application to deformation processing of magnesium alloys. *Acta Materialia* 60(5):2031–2042.
[10] ASM. *Metals Handbook Vol 2: Properties and Selection: Nonferrous Alloys and Special-Purpose Materials*, ASM InternationalMetals Park, Ohio, USA.
[11] Chandrasekar, S., Trumble, K.P., Mann, J.B., Rohatgi, A., and Efe, M., 2022, High-Silicon Steel Strip by Single-Step Shear Deformation Processing, US OSTI Report 1900616, doi:10.2172/1900616.
[12] Dieter GE (1984) *Workability Testing Techniques*, ASM, Metals ParkOhio, USA.
[13] Ouyang G, Chen X, Liang Y, Macziewski C, Cui J (2019) Review of Fe-6.5 wt% Si high silicon steel—a promising soft magnetic material for Sub-kHz application. *Journal of Magnetism and Magnetic Materials* 481:234–250.
[14] Li S, Beyerlein IJ, Bourke MA (2005) Texture formation during equal channel angular extrusion of FCC and BCC materials: comparison with simple shear. *Materials Science and Engineering: A* 394(1–2):66–77.
[15] Issahaq MN, Udupa A, Sugihara T, Mohanty DP, Mann JB, Trumble KP, Chandrasekar S, M'Saoubi R (2022) Enhancing Surface Quality in Cutting of Gummy Metals Using Nanoscale Organic Films. *CIRP Annals* 71(1):93–96.